

Black-hole-regulated star formation in massive galaxies

Ignacio Martín-Navarro^{1,2}, Jean P. Brodie², Aaron J. Romanowsky^{1,3}, Tomás Ruiz-Lara^{4,5} & Glenn van de Ven^{2,6}

¹University of California Observatories, 1156 High Street, Santa Cruz, California 95064, USA. ²Max-Planck Institut für Astronomie, Königstuhl 17, D-69117 Heidelberg, Germany. ³Department of Physics and Astronomy, San José State University, One Washington Square, San Jose, California 95192, USA. ⁴Instituto de Astrofísica de Canarias, E-38205 La Laguna, Tenerife, Spain.

⁵Departamento de Astrofísica, Universidad de La Laguna, E-38200 La Laguna, Tenerife, Spain. ⁶European Southern Observatory, Karl-Schwarzschild-Strasse 2, 85748 Garching bei München, Germany.

18 JANUARY 2018 | VOL 553 | NATURE | 307

© 2018 Macmillan Publishers Limited, part of Springer Nature. All rights reserved.

Hanbyul Jang

UNIST

2018.4.5 Journal Club

LETTER

First Observational evidence

doi:10.1038/nature24999

Black-hole-regulated star formation in massive galaxies

Ignacio Martín-Navarro^{1,2}, Jean P. Brodie², Aaron J. Romanowsky^{1,3}, Tomás Ruiz-Lara^{4,5} & Glenn van de Ven^{2,6}

¹University of California Observatories, 1156 High Street, Santa Cruz, California 95064, USA. ²Max-Planck Institut für Astronomie, Königstuhl 17, D-69117 Heidelberg, Germany. ³Department of Physics and Astronomy, San José State University, One Washington Square, San Jose, California 95192, USA. ⁴Instituto de Astrofísica de Canarias, E-38205 La Laguna, Tenerife, Spain.

⁵Departamento de Astrofísica, Universidad de La Laguna, E-38200 La Laguna, Tenerife, Spain. ⁶European Southern Observatory, Karl-Schwarzschild-Strasse 2, 85748 Garching bei München, Germany.

18 JANUARY 2018 | VOL 553 | NATURE | 307

© 2018 Macmillan Publishers Limited, part of Springer Nature. All rights reserved.

Hanbyul Jang

UNIST

2018.4.5 Journal Club

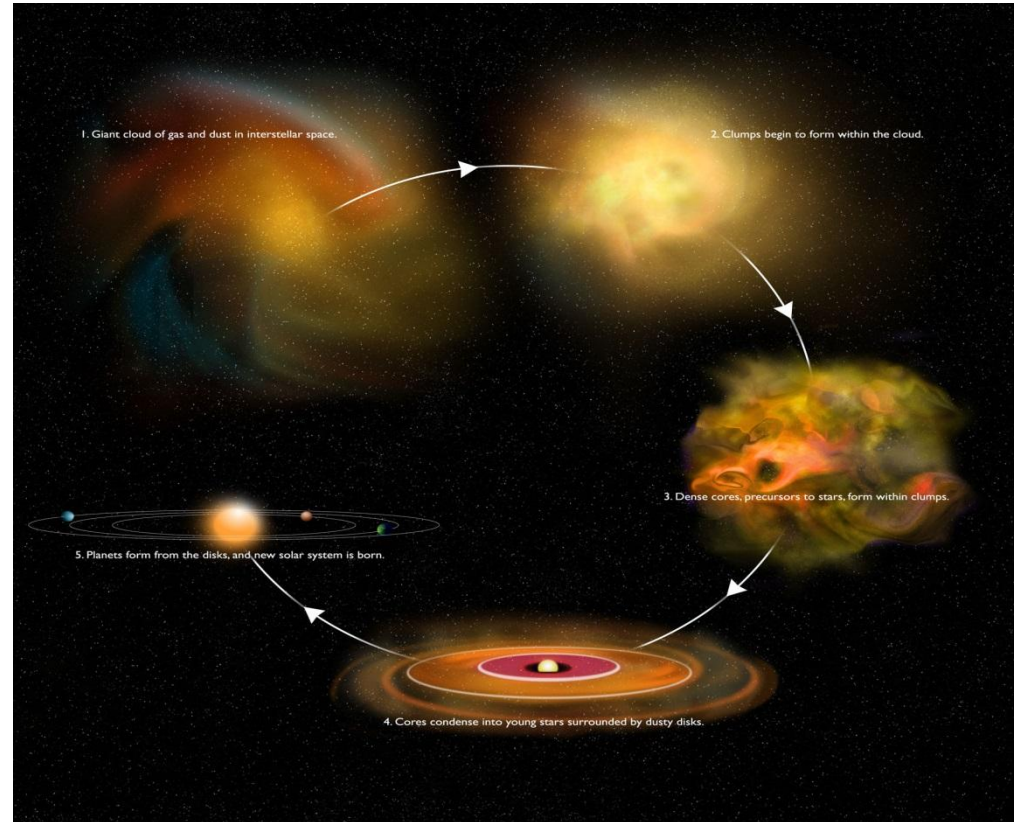
Star Formation in Galaxies



Large Magellan Cloud



Dwarf galaxy ESO 553-46



$$t_{cool} = \frac{3}{2} \frac{nkT}{[n^2 \Lambda(T)]}$$

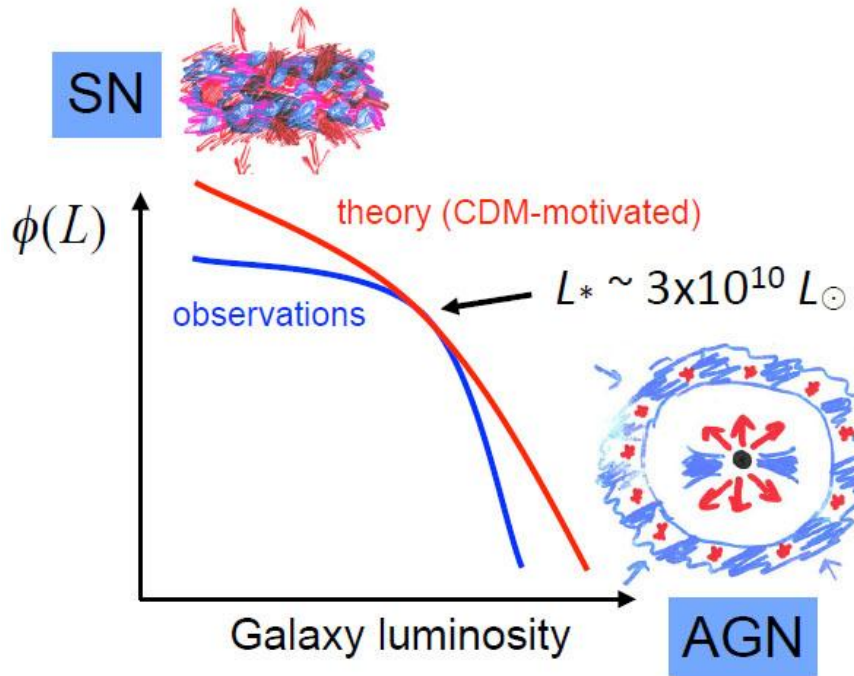
$\Lambda(T)$: cooling function

$$t_{dyn} = \frac{3}{\sqrt{32\pi G\rho}}$$

$$t_{cool} < t_{dyn}$$

To occur star formation, cooling is essential

Star Formation in Galaxies



In an inhomogeneous galactic halo, gas clouds collide at the virial velocity

$$M_{\text{cool}}^* = \frac{\alpha^3}{\alpha_g^2} \frac{m_p}{m_e} \frac{t_{\text{cool}}}{t_{\text{dyn}}} T^{1+2\beta}$$

$$\alpha = e^2/(\hbar c) \quad \alpha_g = Gm_p^2/e^2$$

the electromagnetic and gravitational fine structure constants

$$\Lambda(T) \propto T^\beta \quad (10^5 - 10^7 \text{ K})$$

$\beta \approx -1/2$ for a low metallicity plasma

AGN Feedback is required for massive galaxies

$$\frac{L}{L_\odot} = \left(\frac{M}{M_\odot} \right)^\alpha$$

Mass-Luminosity relation

AGN Feedback



AGN(Active Galactic Nucleus)

A compact region at the center of a galaxy that has a much higher than normal luminosity

The radiation from an AGN is believed to be a result of accretion of matter by a Super-Massive Black Hole at the center of its host galaxy

AGN Feedback

Outflow from the central BH delivers momentum to the protogalactic gas

Eddington luminosity is high enough that residual gas is ejected

Jets and cocoons heat halo gas and inhibit cooling

Numerical Simulation

Wagner et al. 2012 APJL

UFO Feedback

3

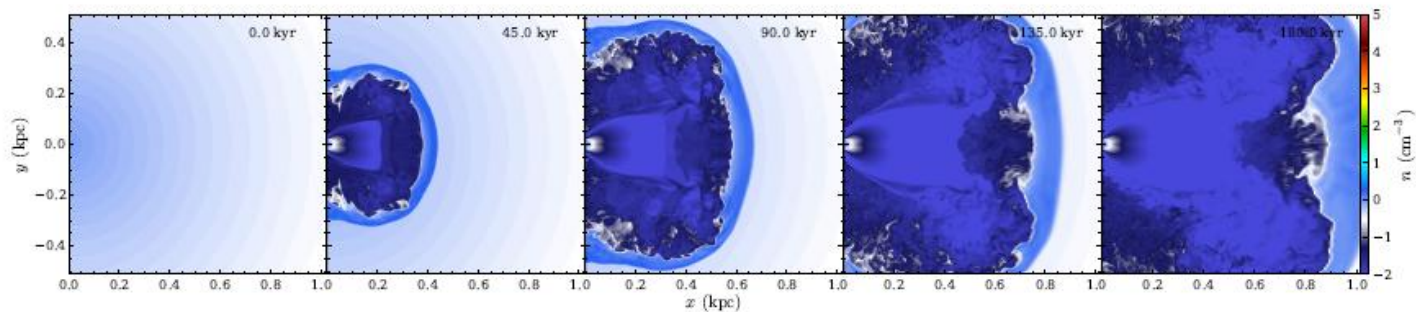


FIG. 1.— Midplane density slices of the evolution of a $10^{44} \text{ erg s}^{-1}$ UFO in an ISM devoid of clouds (Run A). See the electronic edition of the Journal for a color version of this figure.

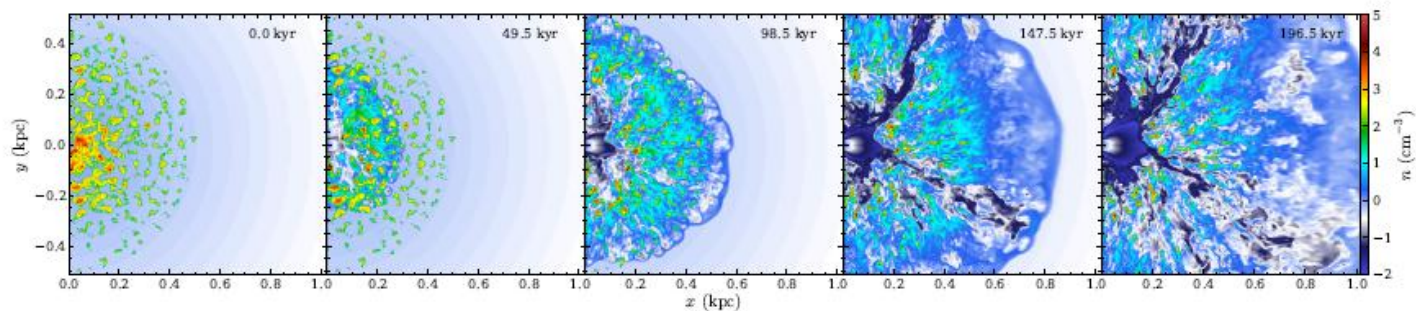


FIG. 2.— Same as Fig 1, but for a two-phase ISM with spherically distributed clouds (Run B).

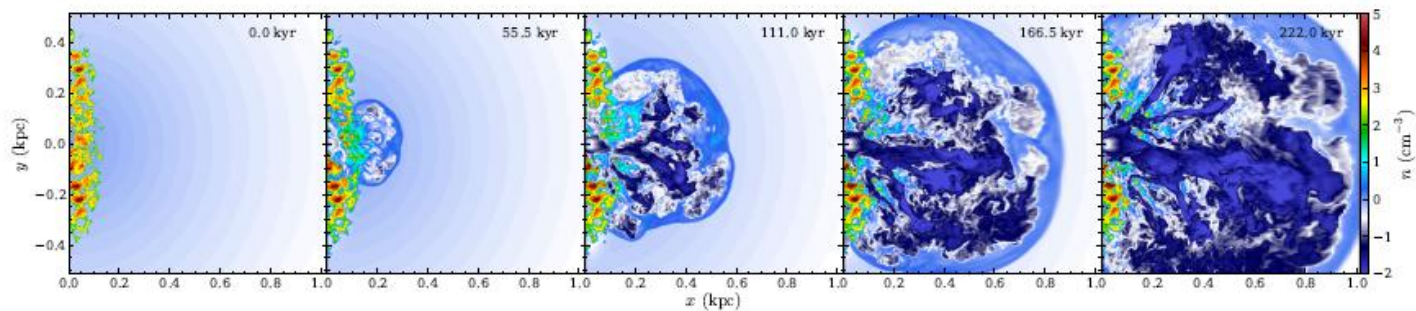


FIG. 3.— Same as Fig 1, but for a two-phase ISM with clouds distributed in a quasi-Keplerian disk (Run C).

Numerical Simulation

The EAGLE project: simulating the evolution and assembly of galaxies and their environments

J. Schaye et al. 2015 MNRAS

4.6 Black holes and feedback from AGN

In our simulations feedback from accreting, supermassive BHs quenches star formation in massive galaxies, shapes the gas profiles in the inner parts of their host haloes, and regulates the growth of the BHs.

Models often make a distinction between ‘quasar’- and ‘radio-mode’ BH feedback (e.g. Bower et al. 2006; Croton et al. 2006; Sijacki et al. 2007), where the former occurs when the BH is accreting efficiently and comes in the form of a hot, nuclear wind, while the radio mode operates when the accretion rate is low compared to the Eddington rate and the energy is injected in the form of relativistic jets. Because cosmological simulations lack the resolution to properly distinguish these two feedback modes and because we want to limit the number of feedback channels to the minimum required to match the observations of interest, we choose to implement only a single mode of AGN feedback with a fixed efficiency. The energy is injected thermally at the location of the BH at a rate that is proportional to the gas accretion rate. Our implementation may therefore be closest to the process referred to as quasar-mode feedback. For OWLS we found that this method led to excellent agreement with both optical and detailed X-ray observations of groups and clusters (McCarthy et al. 2010, 2011; Le Brun et al. 2014).

Our implementation consists of two parts: (i) prescriptions for seeding low-mass galaxies with central BHs and for their growth via gas accretion and merging (we neglect any growth by accretion of stars and dark matter) and (ii) a prescription for the injection of feedback energy. Our method for the growth of BHs is based on the one introduced by Springel, Di Matteo & Hernquist (2005b) and modified by Booth & Schaye (2009) and Rosas-Guevara et al. (2013), while our method for AGN feedback is close to the one described in Booth & Schaye (2009). Below we summarize the main ingredients and discuss the changes to the methods that we made for EAGLE.

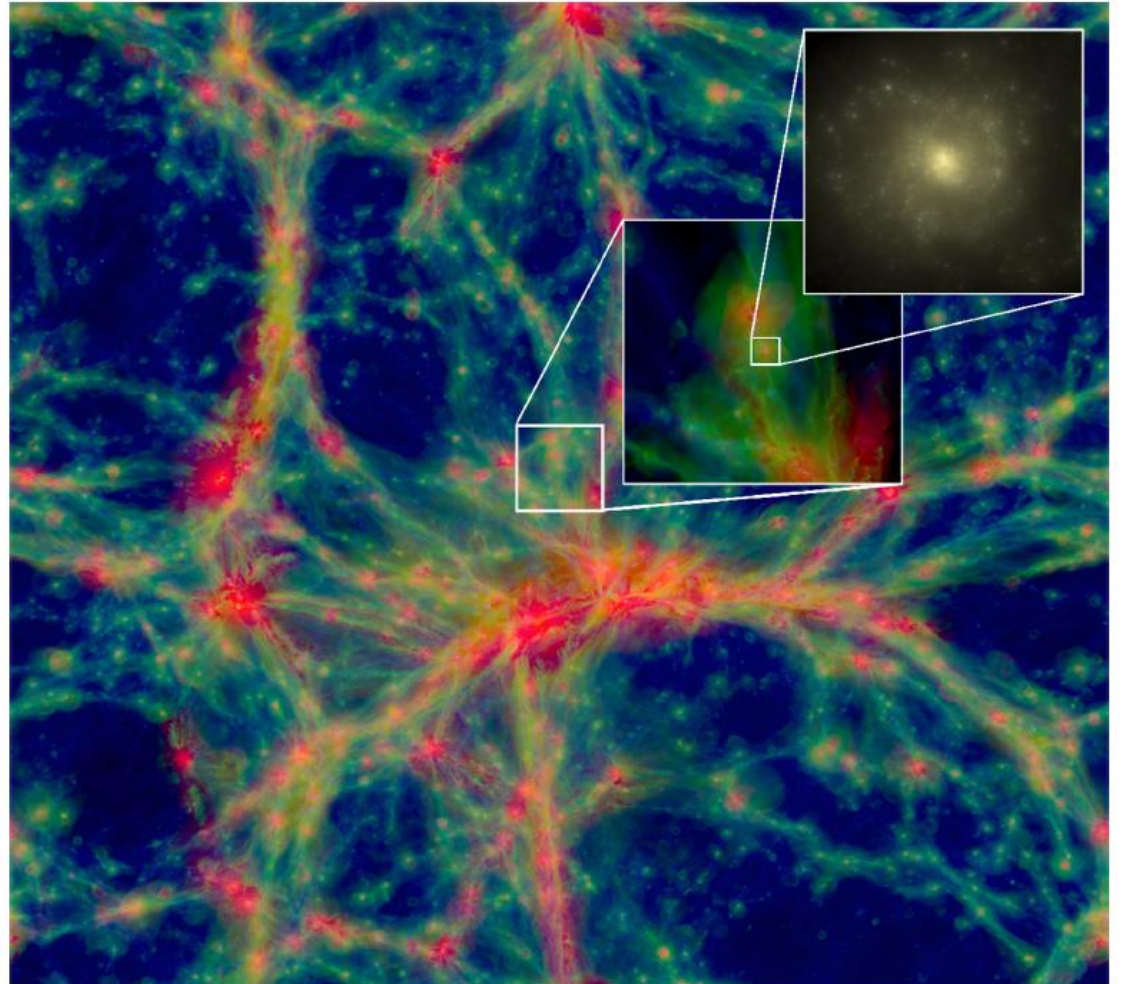
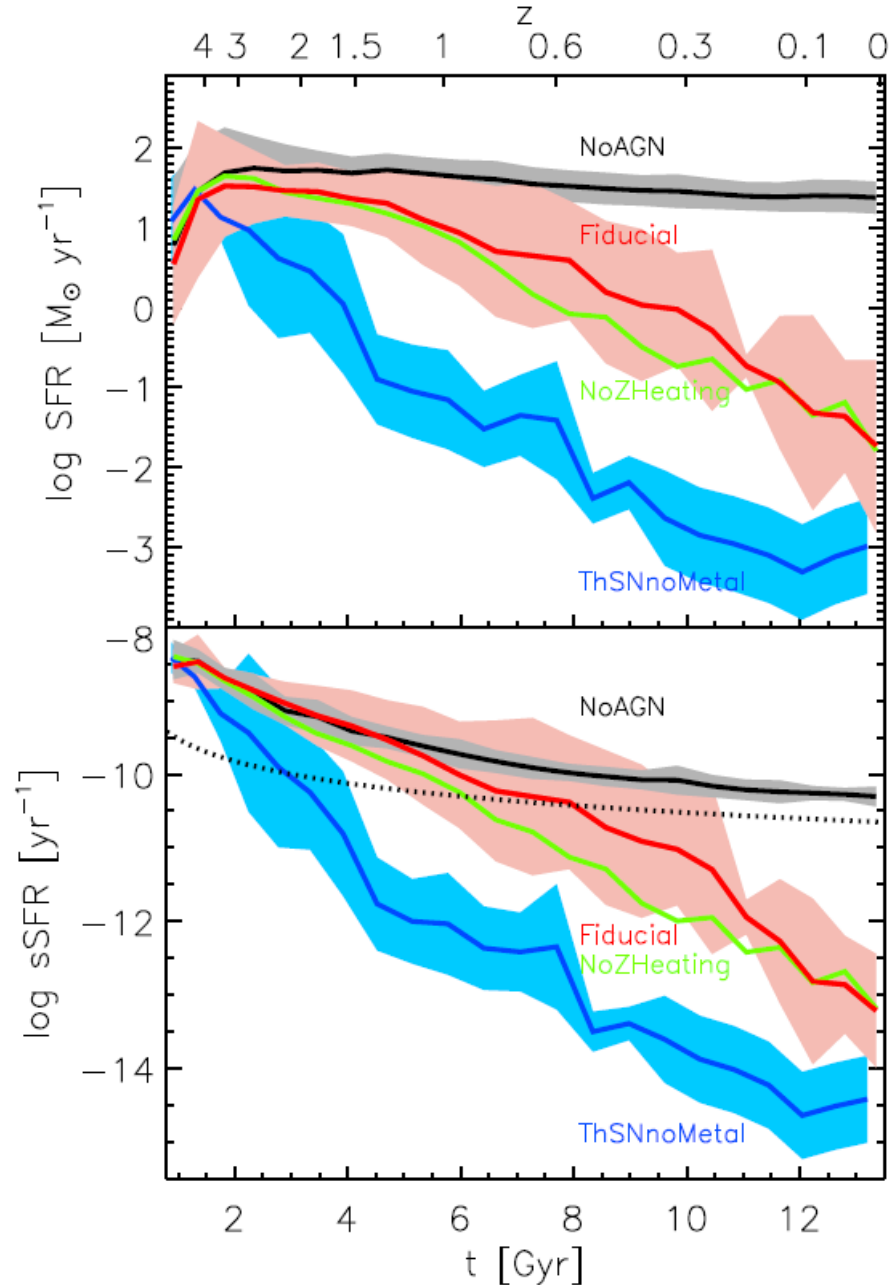


Figure 1. A $100 \times 100 \times 20$ cMpc slice through the Ref-L100N1504 simulation at $z = 0$. The intensity shows the gas density while the colour encodes the gas temperature using different colour channels for gas with $T < 10^{4.5}$ K (blue), $10^{4.5}$ K $< T < 10^{5.5}$ K (green), and $T > 10^{5.5}$ K (red). The insets show regions of 10 cMpc and 60 kpc on a side and zoom into an individual galaxy with a stellar mass of $3 \times 10^{10} M_{\odot}$. The 60 kpc image shows the stellar light based on monochromatic u -, g - and r -band SDSS filter means and accounting for dust extinction. It was created using the radiative transfer code SKIRT (Baes et al. 2011).

Numerical Simulation

Choi et al. 2017 APJ



(1) Fiducial: the reference model that includes all physical modules listed above, i.e., mechanical and radiative AGN feedback, stellar feedback with snowplow SN feedback, metal cooling and enrichment, and the metal heating effect from photoelectric heating and cosmic X-ray background. Feedback-related numerical parameters were calibrated against the black hole mass–stellar velocity dispersion ($M_{\text{BH}} - \sigma_*$) relation and the baryonic conversion rate at $z = 0$ (see Figures 1 and 2).

(2) NoAGN: without black hole and AGN feedback. This model isolates the effect of the AGN feedback.

(3) NoZHeating: same as the fiducial model, but without the new ingredients of metal heating effects listed in Section 2.6, including metallicity-dependent Compton heating, photoelectric heating, and cosmic X-ray background heating.

(4) ThSNnoMetal: from a previous paper (Choi et al. 2015), this model uses thermal SN feedback (Springel & Hernquist 2003) instead of ejective SN feedback described in Section 2.3. This model does not include metal enrichment, metal-induced heating/cooling, and early stellar feedback. Note that we presented 20 halos in Choi et al. (2015), but we have performed 10 more zoom-in simulations for a fair comparison.

Figure 3. Top: averaged star formation rate over time for the 30 central galaxies for different models: fiducial model (red), model without AGN feedback effect (NoAGN; black), model without metal heating effect (NoZHeating; green), and model with thermal SN feedback and without metal enrichment (ThSNnoMetal; blue). The solid lines show the average value, and shaded regions illustrate the 1σ scatter. For clarity of display, the 1σ region of the NoZHeating model is not shown. Bottom: same as in the top panel, but for the median specific star formation rates. The dotted black line indicates the specific star formation rates equal to $0.3/t_H$, a commonly used criterion separating quiescent and star-forming galaxies (e.g., Franx et al. 2008). The NoAGN feedback model (black) stays above this criterion, constantly star-forming throughout the evolution.

Black-hole-regulated star formation in massive galaxies

Ignacio Martín-Navarro^{1,2}, Jean P. Brodie², Aaron J. Romanowsky^{1,3}, Tomás Ruiz-Lara^{4,5} & Glenn van de Ven^{2,6}

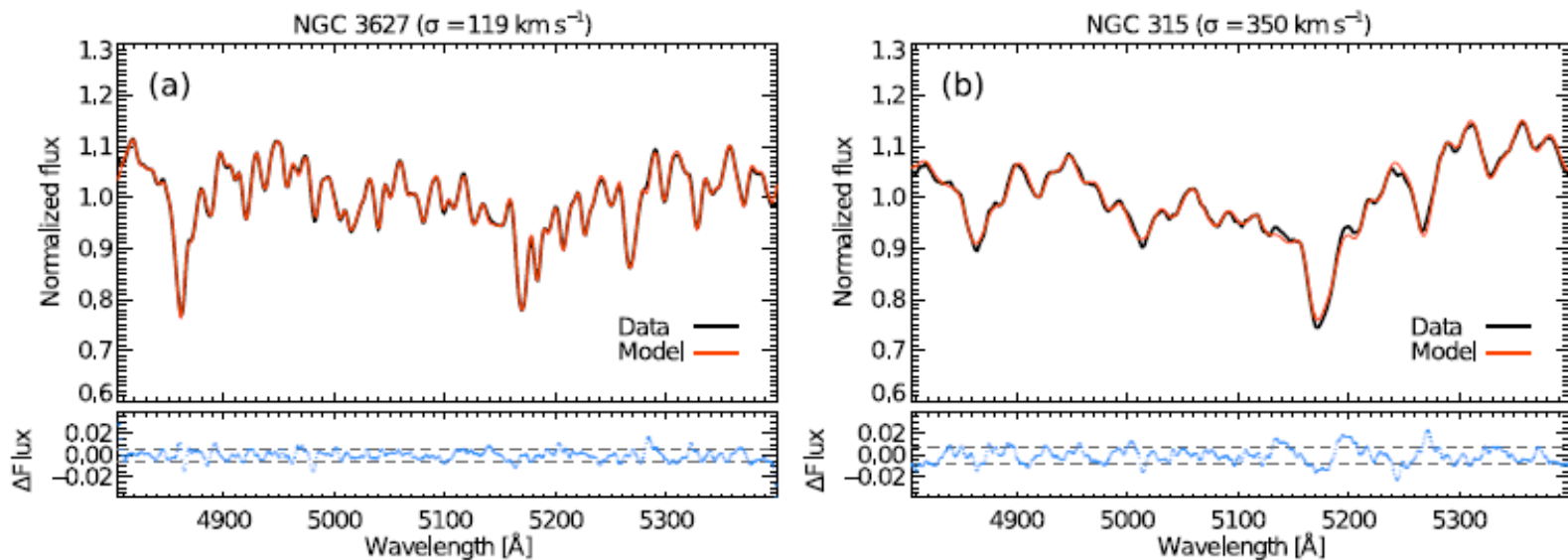
The **first direct observational evidence** of the effect of the **supermassive black hole** on the **star formation history** of the galaxy

Galaxy Data \longrightarrow 74 galaxies ($M: 10^{10} \sim 10^{12} M_{\text{sun}}$)

- Hobby-Eberly Telescope Massive Galaxy Survey (HETMGS)

Star formation history

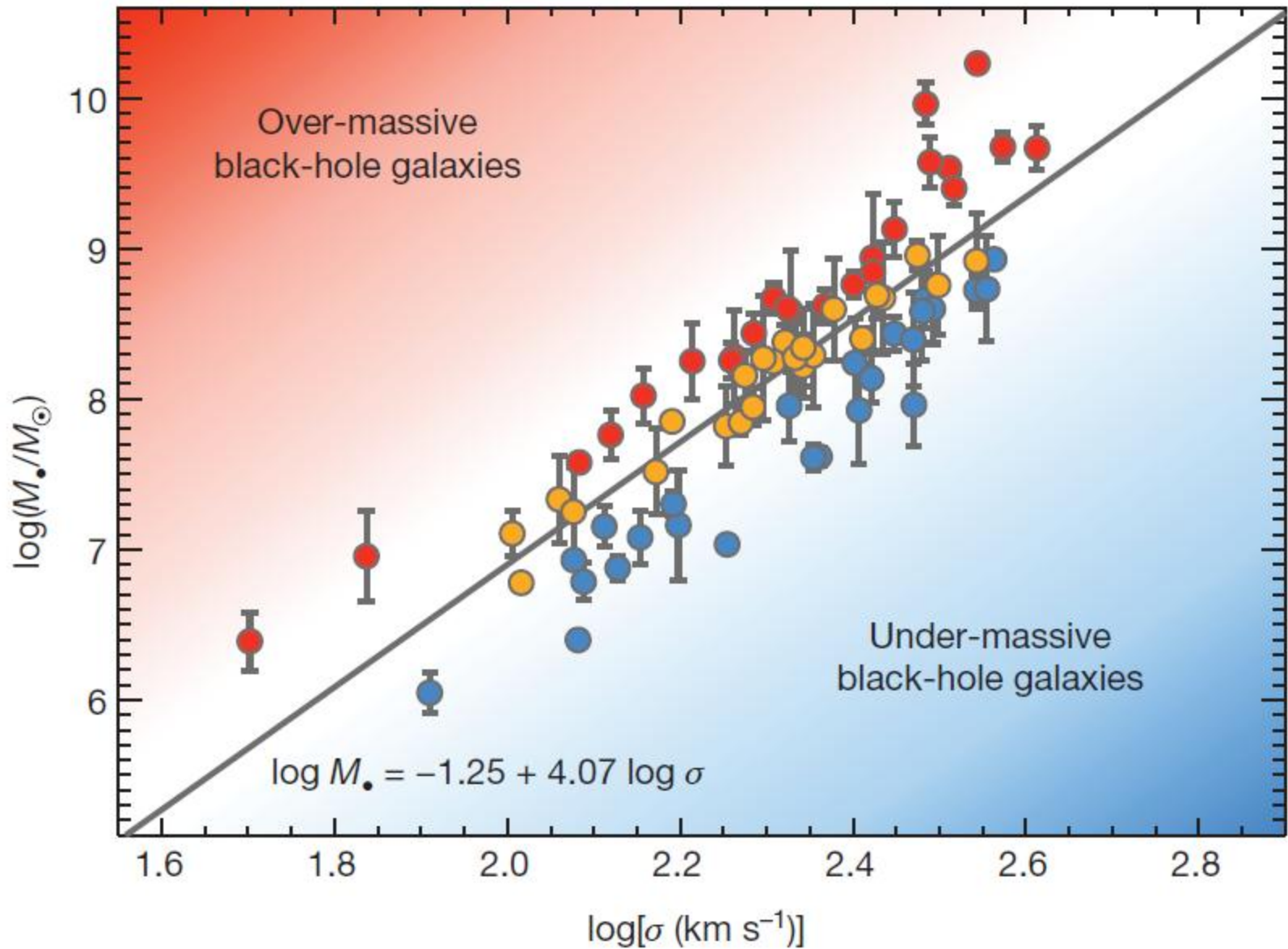
- Stellar Content and Kinematics via Maximum A Posteriori likelihood (STECKMAP) code
- Decompose the observed spectrum of a galaxy as a temporal series of single stellar population models



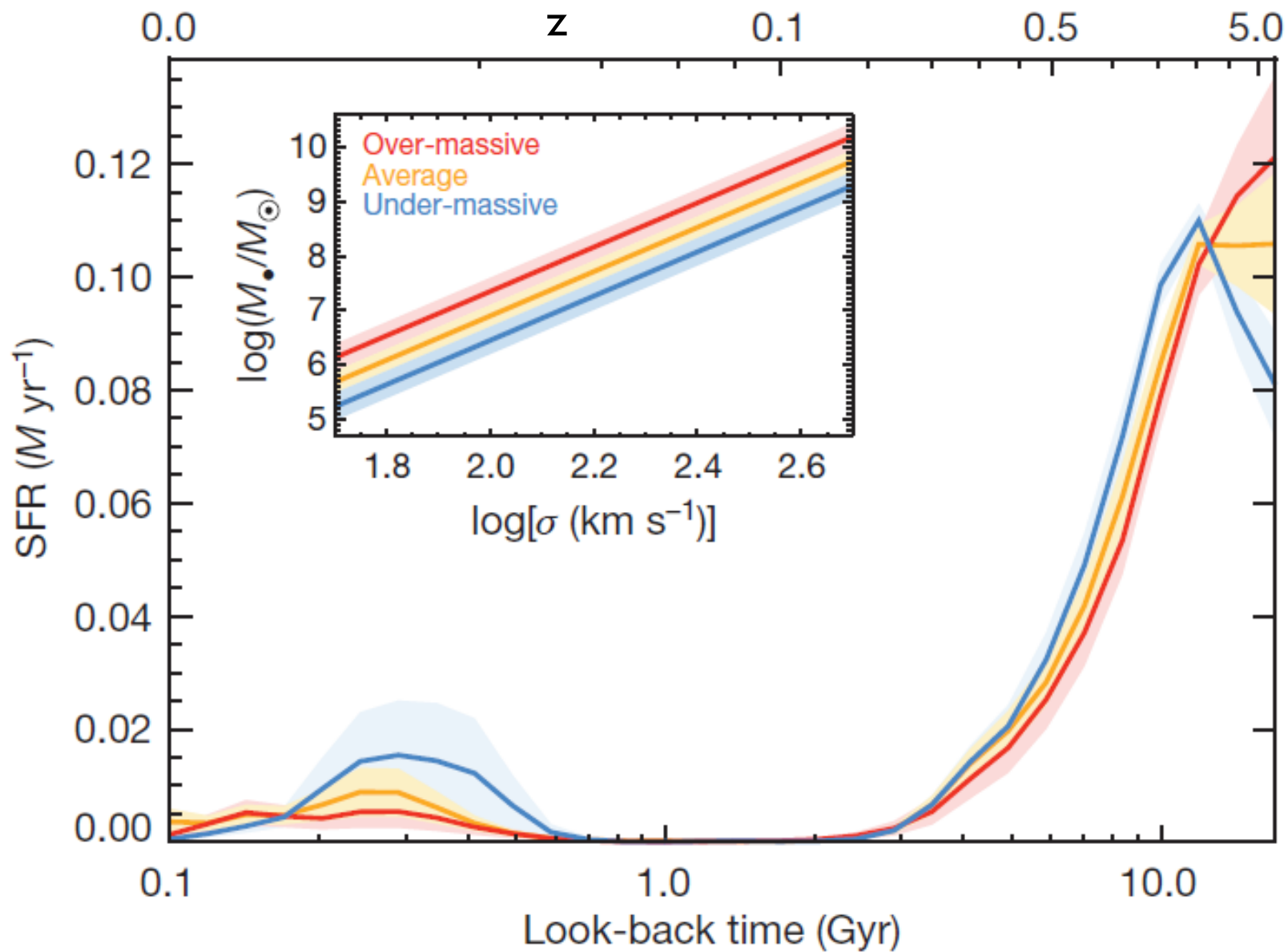
Extended Data Figure 1 | Data and best-fitting stellar populations model. **a**, The spectrum of the low- σ galaxy NGC 3627; **b**, the spectrum of the higher- σ galaxy NGC 315. Along with the HETMGS spectra (black line), we also show the best-fitting STECKMAP model (red line).

In the bottom panel, we show the residuals (blue dots), which are in both cases below 2%. The standard deviation is shown as dashed horizontal lines.

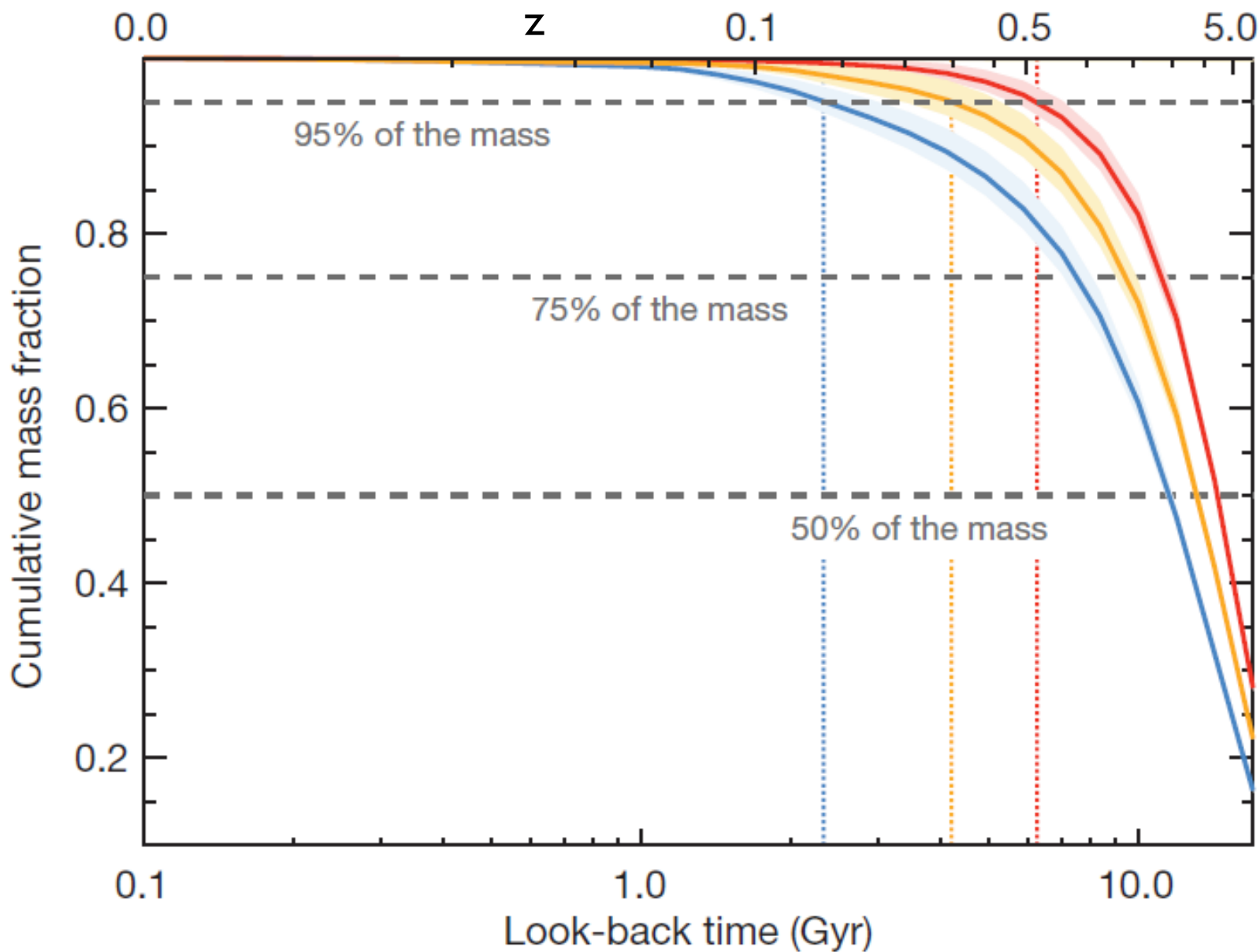
Dispersion relation between black-hole mass and stellar velocity



Evolution of the star formation rate (SFR)



Cumulative mass distribution



Conclusion

Theory & Simulations need the AGN feedback to explain the star formation in the massive galaxies

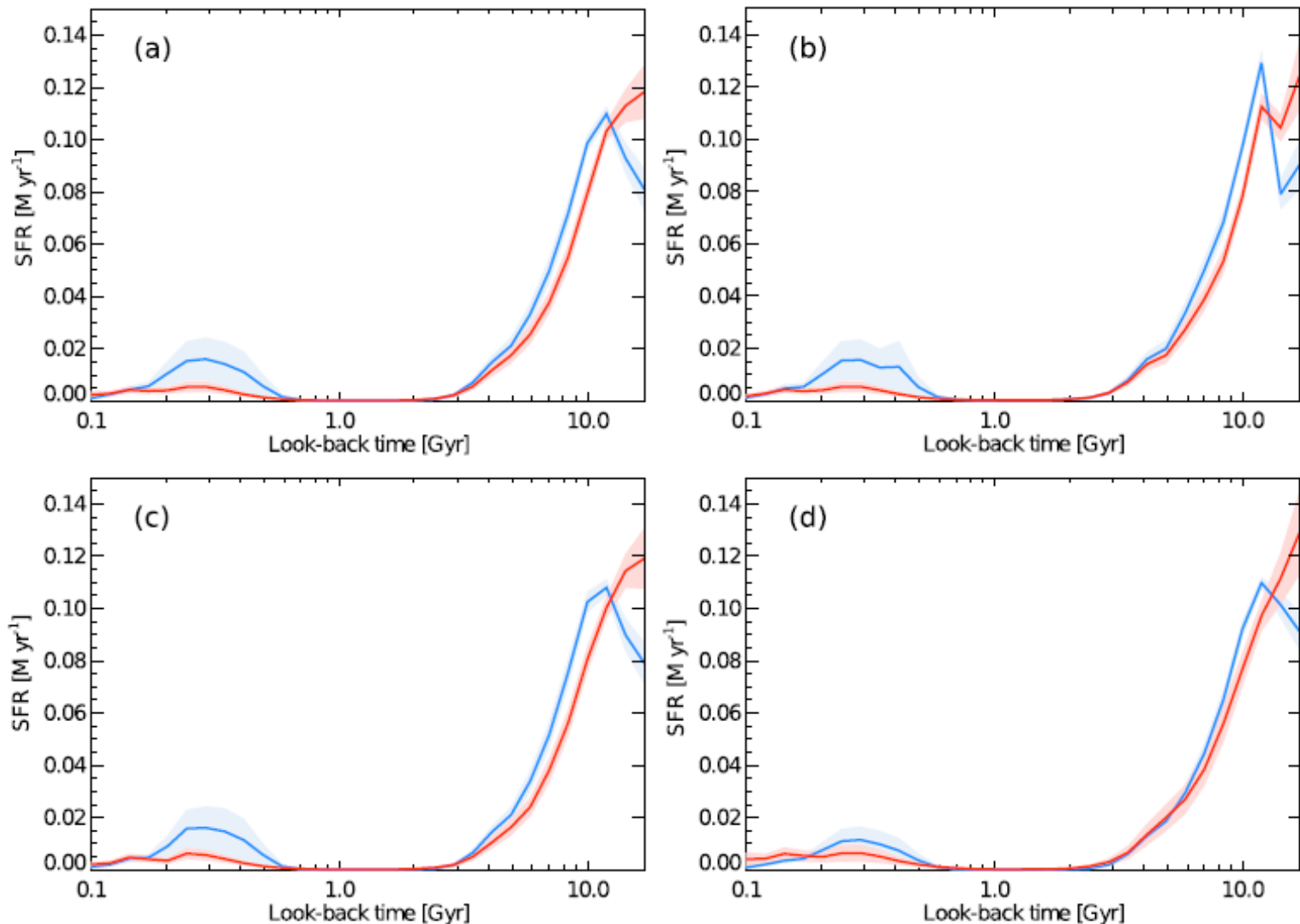
There was no direct observational evidence between the supermassive black hole and the star formation of the host galaxy

They show that the star formation histories of nearby massive galaxies depend on the mass of the central supermassive black hole

Galaxies with over-massive black holes experienced more intense star formation rate in the very early universe

Star formation in over-massive black hole galaxies was quenched earlier

Young stellar populations are more prominent in under-massive black-hole galaxies



Extended Data Figure 3 | Robustness of the recovered star formation rates. Different panels correspond to the different tests performed in order to explore the reliability of our results. As in Fig. 2, red and blue lines indicate the star formation rate (SFR) as a function of look-back time for over-massive and under-massive black-hole galaxies, and the shaded areas mark the 1σ uncertainties. **a.** Our preferred model, as a reference. A two-sided Kolmogorov-Smirnov comparison between over-massive

and under-massive galaxies indicates that the two distributions are significantly different ($P = 0.026$). **b.** Here, we left the regularization of the SFH almost free, by setting $\mu_x = 0.1$. **c.** We varied the regularization of the age-metallicity relation in the same way, changing μ_2 from 10 to 0.1. **d.** Finally, we adopted a different (but inconsistent) $M_x - \sigma$ relation¹² to separate our sample. All these tests demonstrate that our conclusions are insensitive to systematics in the analysis.